

**Local modes of Fe and Co atoms in NiAl intermetallics**

K. Parlinski and P. T. Jochym

*Institute of Nuclear Physics, Polish Academy of Sciences, ul.Radzikowskiego 152, 31-342 Cracow, Poland*

O. Leupold, A. I. Chumakov, and R. Ruffer

*European Synchrotron Radiation Facility (ESRF), B.P.220, F-38043 Grenoble Cedex, France*

H. Schober

*Institute Laue Langevin, B.P. 156, 38042 Grenoble, Cedex 9, France*

A. Jianu

*National Institute for Materials Physics, P.O. Box M.G.07, RO-76900 Bucharest, Romania*

J. Dutkiewicz and W. Maziarz

*Institute of Metallurgy and Materials Science, Polish Academy of Sciences, ul. Reymonta 25, 30-059 Cracow, Poland*

(Received 3 September 2004; published 28 December 2004)

Using nuclear inelastic scattering of synchrotron radiation and inelastic neutron scattering we have investigated the vibrational properties of Fe and Co impurities in NiAl intermetallics, and compared them with the density functional theory calculations. The Fe phonon spectra show two sharp peaks appearing in the frequency gap between the Ni and Al phonon bands, and originating from the local modes of Fe residing in Ni, or Al sublattices. Co, which replaces Ni, vibrates within a narrow frequency interval occurring close to the upper edge, but still within the Ni phonon band. The *ab initio* calculations show that these effects are expected when impurity-host force constants differ from host-host force constants causing a dynamic mismatch between guest and host vibrations.

DOI: 10.1103/PhysRevB.70.224304

PACS number(s): 71.15.Mb, 61.82.Bg

**I. INTRODUCTION**

Vibrations of isolated impurity atoms may strongly differ from those of the host atoms due to different atomic masses and changes in the impurity–host force constants.<sup>1</sup> A local mode may occur above the maximum frequency of the phonon density of states, or in the frequency gap between phonon bands. Usually, a decrease/increase of impurity mass could be replaced by an increase/decrease of impurity-host force constants. It is generally understood that a local mode may arise only when specific conditions between atomic masses and force constants of impurity and host atoms are fulfilled. Otherwise the impurity vibration is not prevented to couple to the host vibrations. In particular, a local mode may appear for atoms with masses reasonably smaller than the mass of the host atoms, provided the force constants do not change. The amplitudes of the local modes rapidly diminish with distance from the impurity atom. Being able to rationalize from simple principles the way vibrational amplitudes are confined in space is of prime importance for the general understanding of disordered systems including glasses and their transport properties.

An analysis and measurements of local modes have already been done in the past.<sup>2</sup> For example, by inelastic neutron scattering, local phonon modes have been found above the maximal frequency of the host phonon density of states for Li impurities in a Mg crystal, and for Be impurities in a Cu crystal,<sup>3</sup> indicating a decrease of impurity-host force constants. The vibrational density of states of highly dilute Fe in Al or Fe in Cu metals were measured by nuclear inelastic

scattering of synchrotron radiation.<sup>4</sup> In Al the Fe vibrations are in resonance with all the host modes. In the case of Fe in Cu metal, in addition to the resonance vibrations, a local mode above the maximal frequency was observed. A comparison with the theory of Mannheim<sup>5</sup> established an increase of impurity-host force constants with respect to those of the host lattice.

We demonstrate below that in the same system one finds two local modes in the gap of phonon density of states, i.e., within the frequencies of forbidden phonons: one originating from large impurity-host force constant, and a second coming from the mass defect. Moreover, in another crystal we show that a local mode of the impurity atom with a negligible mass defect may persist in the allowed frequency band of the host atoms, and that this effect is caused by the change of impurity-host force constants.

**II. AB INITIO CALCULATIONS**

The *ab initio* calculations of NiAl, Ni<sub>43.75</sub>Fe<sub>6.25</sub>Al<sub>50</sub>, Ni<sub>50</sub>Al<sub>43.75</sub>Fe<sub>6.25</sub> and Ni<sub>43.75</sub>Co<sub>6.25</sub>Al<sub>50</sub> structures were performed within the density functional theory, using the PAW potentials<sup>6,7</sup> and the generalized gradient approximation (GGA), as implemented in the VASP software.<sup>8,9</sup> The NiAl crystallizes in the primitive cubic structure, space group Pm $\bar{3}$ m [Ni: (0,0,0), Al: ( $\frac{1}{2}, \frac{1}{2}, \frac{1}{2}$ )], with experimental and calculated lattice constants equal to  $a=2.886$  Å and  $a=2.8921$  Å,<sup>10</sup> respectively. In all phonon calculations we have used the  $2 \times 2 \times 2$  supercells with 16 atoms, in which one atom, if needed, was replaced either by Fe or Co. The

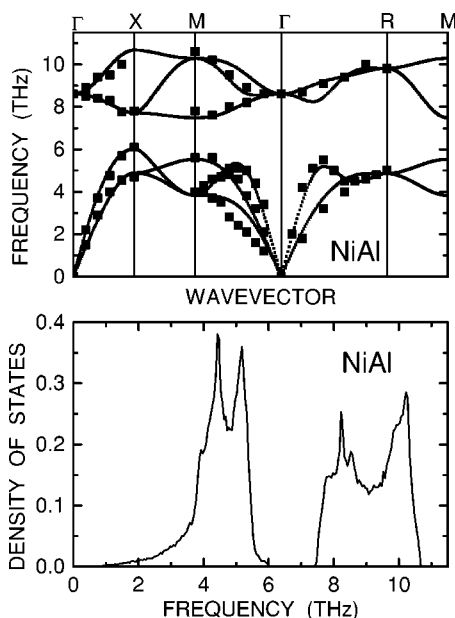


FIG. 1. *Ab initio* calculated (a) phonon dispersion relations of NiAl. Experimental points are taken from Ref. 13. (b) Phonon density of states of NiAl.

wavevector summation over electronic states was confined to  $\#\mathbf{k}: 6 \times 6 \times 6$  mesh. The phonon dispersion curves, and hence the density of states, were determined by the direct method.<sup>11,12</sup> The Hellmann-Feynman forces were calculated for symmetry independent displacement with the amplitude of 0.03 Å.

First, the phonons were obtained in stoichiometric intermetallic NiAl. The calculated phonon dispersion relations are compared in Fig. 1(a) with the neutron scattering measurements.<sup>13</sup> They agree also very well with another *ab initio* calculation.<sup>14</sup> The calculated phonon density of states, Fig. 1(b), consists of two bands: Ni at low- and Al at high-frequency intervals spreading from 0.0 to 6.05 THz, and from 7.50 to 10.70 THz, respectively.

### III. NiAl WITH IRON IMPURITY

Polycrystalline sample of NiAl alloy with 1 at.%  $^{57}\text{Fe}$  was prepared from high purity elements by arc-melting in a water cooled copper hearth using a nonconsumable tungsten electrode under purified argon atmosphere. To increase homogeneity, the ingot was reversed and re-melted several times. It was subsequently encapsulated in a quartz tube under vacuum and subjected to heat treatment at 1073 K for 6 days. The specimen was quenched in cold water without breaking the ampoule. Nuclear inelastic scattering spectra of iron in NiAl with 1 at.% Fe were measured by the nuclear inelastic scattering technique<sup>15</sup> at the Nuclear Resonance beam line ID18<sup>16-18</sup> at ESRF, Grenoble, France. The spectra were measured at room temperature (294 K) with an energy resolution of 0.13 THz. The photon flux on the sample was about  $0.7 \times 10^9$  photons per second, and the measuring time amounts to 29 hours. The Lamb-Mössbauer factor was 0.77(1). The instrumental function of the setup was deter-

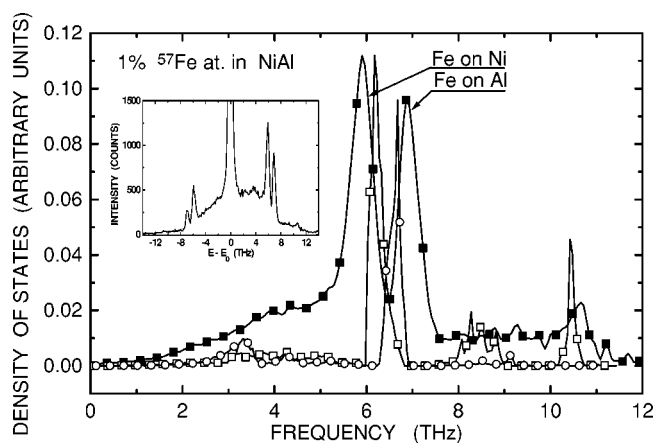


FIG. 2. Solid squares: measured phonon density of states of  $^{57}\text{Fe}$  in NiAl alloy with 1 at.% Fe. Error bars are as large as the square points. Open squares: *ab initio* calculated partial phonon density of states of Fe on the Ni sublattice. Open circles: *ab initio* calculated partial phonon density of states of Fe on the Al sublattice. The inset shows the nuclear inelastic scattering data from  $^{57}\text{Fe}$  in a NiAl alloy with 1 at.% Fe.

mined by several scans in nuclear forward scattering geometry from a  $^{57}\text{Fe}$  foil before, during and after the inelastic scans on the sample.

The phonon density of states of  $^{57}\text{Fe}$  in NiAl with 1 at.% Fe extracted from the nuclear inelastic scattering is shown in Fig. 2. There are two sharp peaks observed at 5.90 THz and 6.90 THz, and a small peak close to 10.66 THz. Similar sharp peaks have been obtained from *ab initio* calculations, Fig. 3, for a Fe atom placed in the supercell center and surrounded either by Al, or Ni atoms, thus representing ordered  $\text{Ni}_{43.75}\text{Fe}_{6.25}\text{Al}_{50}$  or  $\text{Ni}_{50}\text{Al}_{43.75}\text{Fe}_{6.25}$  models, respectively. The calculated Fe partial phonon density of states consist of sharp peaks at 6.20 THz and 6.68 THz for Fe in Ni and Al sublattices, respectively. These peak positions deviate from the measured ones by 0.30 THz and  $-0.22$  THz, respectively. The lower frequency mode belongs to Fe vibrating within the Ni sublattice. It appears as a local mode due to a remarkable increase of the impurity-host force constants with respect to the host-host interactions, in spite of the fact that the Fe and Ni masses are almost the same. The higher frequency local mode belongs to Fe vibrating within the Al sublattice. This local mode splits down from the optical band edge belonging mainly to Al vibrations. In this case the impurity-host force constants remain comparable to the host-host force constants, however, the mass ratio  $M_{\text{Fe}}/M_{\text{Al}}$  is close to 2.

The small deviations between measured and calculated peak positions could come from a different neighborhood at the distances greater than the supercell size. In the *ab initio* calculations, due to the periodic boundary conditions, Fe atoms are separated by distances corresponding to the supercell lattice constants, while in the measured sample Fe atoms are further apart and randomly distributed. The direct method of phonon calculations uses the cummulant force constants,<sup>11</sup> which are the sum of the corresponding force constants in the original supercell and all its images. In calculations the impurity force constants between the origin supercell and its

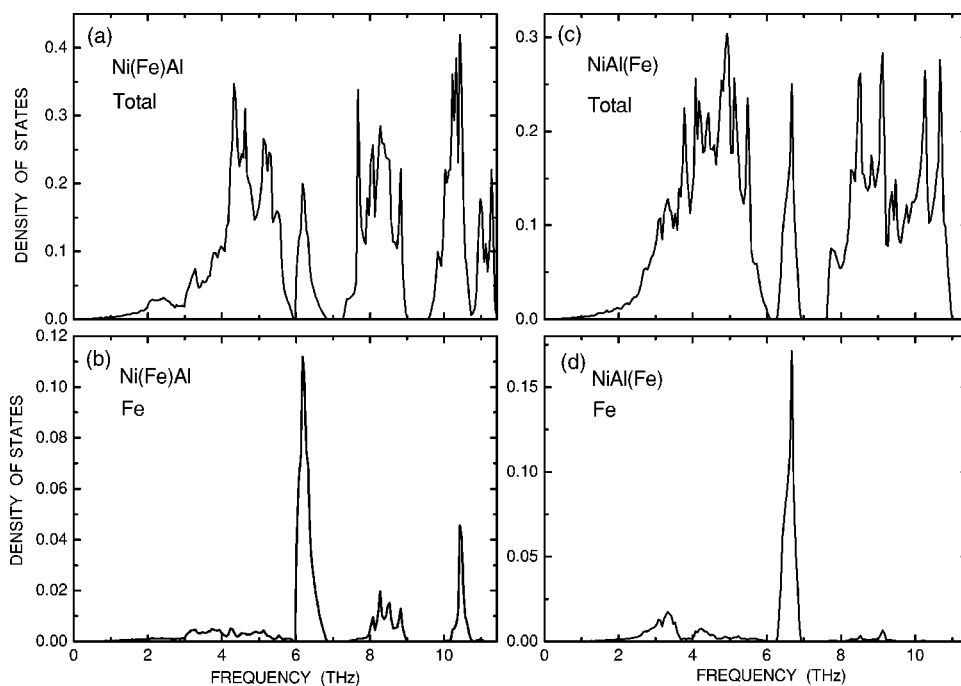


FIG. 3. *Ab initio* calculated (a) total phonon density of states of  $\text{Ni}_{43.75}\text{Fe}_{6.25}\text{Al}_{50}$ ; (b) Fe partial phonon density of states of  $\text{Ni}_{43.75}\text{Fe}_{6.25}\text{Al}_{50}$ ; (c) total density of states of  $\text{Ni}_{50}\text{Al}_{43.75}\text{Fe}_{6.25}$ ; (d) Fe partial density of states of  $\text{Ni}_{50}\text{Al}_{43.75}\text{Fe}_{6.25}$  supercells.

image could be of Fe-Fe type, while in the measured sample the force constants at the same distance are of Fe-Ni, or Fe-Al types, and therefore should be different. We have estimated that a change of force constants between Fe atoms belonging to original supercell and its closest image by about 0.7% (with respect to the on-site force constant) would be sufficient to shift the calculated local modes to their measured values. Moreover, the local mode at (6.20  $\rightarrow$  5.90) THz enters already into the Ni phonon band. It can be shown that due to the increased interaction of Fe atoms with the crystal lattice the local mode at 5.90 THz is accompanied with a noticeable increase of phonon density of states in the region from a 2 THz to 6 THz region, as seen in Fig. 2. A similar enhancement is reported below for Co impurity in Ni sublattice, Fig. 4.

It is well-known that if the impurity atoms have masses similar to those of the host atoms, then they oscillate in the same frequency range as the host atoms, provided the force constants do not change. In the present case the Fe atoms, replacing Ni, are only 5% lighter, and nevertheless they form a local mode that splits-off from the high-frequency Ni phonon band edge towards the phonon gap. The splitting is caused by a 68% increase of impurity on-site force constants, Table I. Simultaneously, the impurity on-site force constant of the Fe atom, which replaces Al, is only 7% smaller than that of Al, Table I. However, combined with an Fe mass, twice as large as that of Al, it leads to a splitting-off of an Fe local mode from the low-frequency edge of the Al band to the phonon gap.

#### IV. NiAl WITH COBALT IMPURITY

The NiAl,  $\text{Ni}_{43.75}\text{Co}_{6.25}\text{Al}_{50}$  and  $\text{Ni}_{40}\text{Co}_{10}\text{Al}_{50}$  alloys have been prepared from 99.9% purity elements by induction melting and casting into the steel mold under argon atmo-

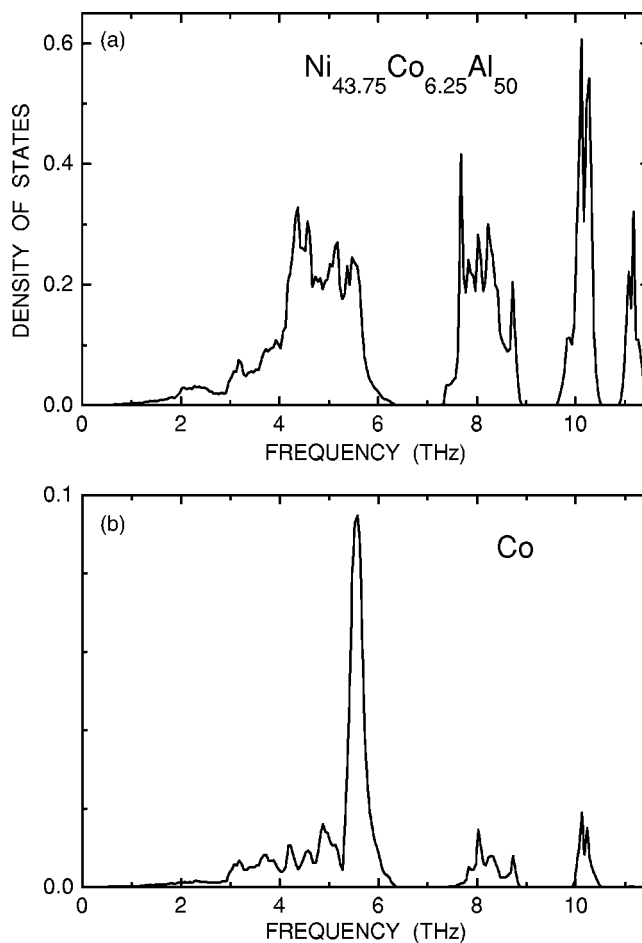


FIG. 4. *Ab initio* calculated (a) total phonon density of states, and (b) Co partial phonon density of states of  $\text{Ni}_{43.75}\text{Co}_{6.25}\text{Al}_{50}$  supercell.

TABLE I. The largest force constant parameters as calculated from VASP and PHONON softwares. The  $A(X)B$  denotes the 16 atomic cubic supercell in which one A-type atom was replaced by an X impurity atom. Notice that for the NiAl(Fe) supercell the atomic names have been interchanged. The  $\Phi_{ij}^{(AB)}(\mathbf{n}, \mathbf{m})$  is the element of the  $3 \times 3$  force constant matrix between A and B atoms located at  $\mathbf{n}$  and  $\mathbf{m}$  sites. The indices  $ij$  run over  $xx, xy, \dots, zz$ . Force constant parameters are in  $\text{eV}/\text{\AA}^2$ .

$A(X)B$	$\Phi_{xx}^{(AA)}(0,0)$	$\Phi_{xx}^{(BB)}\left(\frac{1}{4}, \frac{1}{4}\right)$	$\Phi_{xy}^{(BB)}\left(\frac{1}{4}, \frac{1}{4}\right)$	$\Phi_{xx}^{(AB)}\left(0, \frac{1}{4}\right)$
Ni(Ni)Al	6.51	8.51	0.0	-0.70
Ni(Co)Al	6.57	8.74	0.06	-0.71
Ni(Fe)Al	6.65	8.82	0.21	-0.72
Al(Fe)Ni	8.96	6.63	-0.12	-0.67

$A(X)B$	$\Phi_{xy}^{(AB)}\left(0, \frac{1}{4}\right)$	$\Phi_{xx}^{(XX)}(0,0)$	$\Phi_{xx}^{(XB)}\left(0, \frac{1}{4}\right)$	$\Phi_{xy}^{(XB)}\left(0, \frac{1}{4}\right)$
Ni(Ni)Al	-0.68	6.51	-0.70	-0.68
Ni(Co)Al	-0.69	8.52	-0.84	-0.71
Ni(Fe)Al	-0.72	11.15	-0.99	-0.82
Al(Fe)Ni	-0.69	8.35	-0.75	-0.76

sphere. The homogenization was performed in evacuated quartz ampoules at temperature of 1000 °C for 4 hours and then the samples were slowly cooled. Since the *ab initio* calculations<sup>10</sup> indicated that the formation energies of Co defect in Ni sublattice (1.3 meV/atom) is much smaller than the formation energy of Co in Al sublattice (88.7 meV/atom) we may assume that Co replaces Ni in the NiAl alloy. The inelastic neutron scattering measurements were performed at an ambient temperature on the cold time-of-flight spectrometer IN6 of the ILL, Grenoble, France.<sup>19</sup> The incident wavelength was 4.12 Å, and neutrons were detected over the scattering angles from 13° to 114°. The elastic resolution was determined as 0.073 THz. Measuring time was 6 hours per sample. Using the incoherent approximation<sup>20</sup> the spectra were converted into a neutron weighted phonon density of states, where contributions to the vibrations from each element Ni, Co, Al are taken into account with the weight equal to the total neutron scattering cross-sections, i.e., to 12:4:1, respectively. Multiphonon corrections were performed self-consistently. The measured neutron weighted phonon density of states of NiAl shows that the phonon gap spreads from 6.05 THz to 7.40 THz, which agrees very well with the *ab initio* results.

A little less pronounced local mode appears in the  $\text{Ni}_{43.75}\text{Co}_{6.25}\text{Al}_{50}$  alloy, where some Ni atoms are replaced by Co. As follows from the *ab initio* calculations, the Co vibrations are mostly confined to a single peak placed close to the high-frequency edge of the Ni band, Fig. 4. The Co and Ni masses are almost equal. But 30% larger on-site force constants for Co, Table I, remove the possibility of common vibrations of Ni and Co atoms in the whole Ni band. Figure 4(b) indicates that Co weakly participates in the remaining modes of the crystal.

Three alloys NiAl,  $\text{Ni}_{43.75}\text{Co}_{6.25}\text{Al}_{50}$  and  $\text{Ni}_{40}\text{Co}_{10}\text{Al}_{50}$  have been measured by neutron spectroscopy; see the inset in Fig. 5. The derived neutron weighted density of states are normalized to each other in the frequency interval between

7.50 to 10.70 THz, which corresponds mainly to the Al vibrations, because there, due to the same concentration, the Al density of states should be similar. In Fig. 5 we draw the difference between the intensities  $I$  of the doped and pure specimen ( $I[\text{Ni}_{1-x}(\text{Co}_x)\text{Al}] - I[\text{NiAl}]$ ). They show that the changes introduced by Co lead to the same effects in calculated and measured differences. The observed positive difference in vicinity to 5.5 THz at the high-frequency edge of the Ni phonon band manifests the Co local mode.

Due to a large neutron scattering cross-section of Ni, it would be easier to perform the inelastic neutron scattering measurements on Ni impurities in CoAl alloy, then on Co in NiAl crystal as we have done. However, our *ab initio* calculations show that the Ni impurities in Co sublattice of CoAl

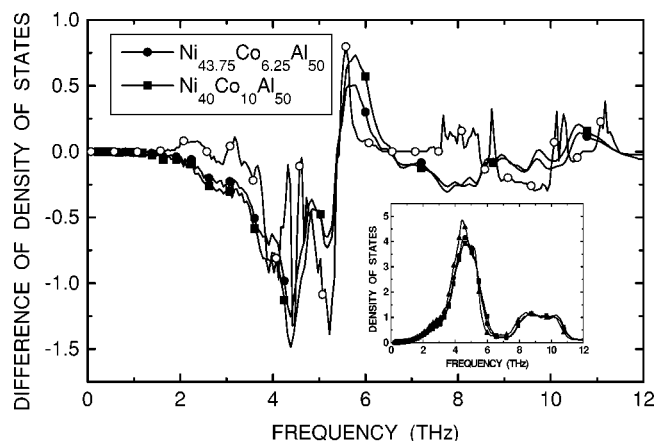


FIG. 5. The neutron weighted intensity differences ( $I[\text{Ni}_{1-x}(\text{Co}_x)\text{Al}] - I[\text{NiAl}]$ ) measured by neutron scattering for  $\text{Ni}_{43.75}\text{Co}_{6.25}\text{Al}_{50}$  (solid circles) and  $\text{Ni}_{40}\text{Co}_{10}\text{Al}_{50}$  (solid squares). Open circles: the same difference obtained from *ab initio* calculations for  $\text{Ni}_{43.75}\text{Co}_{6.25}\text{Al}_{50}$  model. The inset shows the neutron weighted density of states for three samples. The solid triangles denote the NiAl specimen.

crystal do not form local modes. It appears so because the Ni impurity on-site force constant is about 21% smaller than the host Co on-site force constant. This difference causes that the Ni vibrational frequencies are distributed over the whole Co partial phonon density of state spectrum.

## V. CONCLUSIONS

In conclusion, the phonon properties of the intermetallics NiAl with impurity atoms Fe and Co have been measured by the nuclear inelastic scattering, neutron spectroscopy, and calculated within the density functional theory. We found an exceptional case in which Fe impurity atoms, occupying two sublattices in the same crystal, create two local modes with different frequencies occurring in the phonon gap. The masses of Fe and Ni are similar, hence the local mode of Fe in Ni sublattice is caused by much larger Fe force constants. The local mode of Fe in Al sublattice follows mainly from the twice larger Fe mass when compared to Al. Due to combination of neutron scattering measurements and *ab initio* calculations, we could provide evidence that Co atoms create

a narrow local peak within the frequency band of the Ni host atoms, although the mass difference of Co and Ni is negligible. The results show that the phonon density of states probed by a dilute impurity, even when impurity and host atoms are of comparable masses, may dramatically differ from the phonon density of states of the host atoms. Generally, the guest atoms may vibrate more or less decoupled from the host and this even in cases where the frequencies overlap. Such vibrational localization has influence on thermodynamic and transport properties. Being able to rationalize these phenomena in the rather simple case of diluted impurities seems paramount to understanding the dynamics of more complex disordered systems.

## ACKNOWLEDGMENTS

The authors would like to thank J. Korecki for providing us with the enriched  $^{57}\text{Fe}$  isotope. This work was partially supported by the State Committee of Scientific Research (KBN), Grant No. PBZ-KBN-041/T08/01-06, and by BMBF Grant No. 05 KS1PPB/3.

- 
- <sup>1</sup>A. A. Maradudin, E. W. Montroll, and G. H. Weiss, *Theory of Lattice Dynamics in the Harmonic Approximation* (Academic Press, New York, 1963).
- <sup>2</sup>P. H. Dederichs and R. Zeller, *Dynamical Properties of Point Defects in Metals* (Springer-Verlag, Berlin, 1979).
- <sup>3</sup>I. Natkaniec, K. Parlinski, A. Bajorek, and M. Sudnik-Hryniewicz, Phys. Lett. A **24**, 517 (1967).
- <sup>4</sup>M. Seto, Y. Kobayashi, S. Kitao, R. Haruki, T. Mitsui, Y. Yoda, S. Nasu, and S. Kikuta, Phys. Rev. B **61**, 11 420 (2000).
- <sup>5</sup>P. D. Mannheim, Phys. Rev. B **5**, 745 (1972).
- <sup>6</sup>P. E. Blöchl, Phys. Rev. B **50**, 17 953 (1994).
- <sup>7</sup>G. Kresse and D. Joubert, Phys. Rev. B **59**, 1758 (1999).
- <sup>8</sup>G. Kresse and J. Hafner, Phys. Rev. B **47**, 558 (1993); G. Kresse and J. Hafner, *ibid.* **49**, 14 251 (1994).
- <sup>9</sup>G. Kresse and J. Furthmüller, Software VASP, Vienna, 1999; Phys. Rev. B **54**, 11 169 (1996); Comput. Mater. Sci. **6**, 15 (1996).
- <sup>10</sup>K. Parlinski, P. T. Jochym, R. Kozubski, and P. Oramus, Intermetallics **11**, 157 (2003).
- <sup>11</sup>K. Parlinski, Z.-Q. Li, and Y. Kawazoe, Phys. Rev. Lett. **78**, 4063 (1997); Phys. Rev. B **61**, 272 (2000).
- <sup>12</sup>K. Parlinski, PHONON software, Cracow, 2003, <http://wolf.ifj.edu.pl/phonon/>
- <sup>13</sup>M. Mostoller, R. M. Nicklow, D. M. Zehner, S. C. Lui, J. M. Mundenar, and E. W. Plummer, Phys. Rev. B **40**, 2856 (1989).
- <sup>14</sup>G. J. Ackland, X. Huang, and K. M. Rabe, Phys. Rev. B **68**, 214104 (2003).
- <sup>15</sup>E. Gerdau and H. DeWaard, Hyperfine Interact. **123–125** (1999/2000).
- <sup>16</sup>R. Ruffer and A. Chumakov, Hyperfine Interact. **97/98**, 589 (1996).
- <sup>17</sup>A. Chumakov and R. Ruffer, Hyperfine Interact. **113**, 59 (1998).
- <sup>18</sup><http://www.esrf.fr/UsersAndScience/Experiments/HRRS/NRG/>
- <sup>19</sup><http://www.ill.fr/>
- <sup>20</sup>H. Schober, A. Tölle, B. Renker, R. Heid, and F. Gompf, Phys. Rev. B **56**, 5937 (1997); **68**, 214104 (2003).